中国激光

光子晶体面发射蓝光激光器的高速调制性能分析

周扬，贺树敏，沈威，刘启发*

南京邮电大学通信与信息工程学院，江苏 南京 210003

摘要 光子晶体面发射激光器基于光子晶体能带带边模式，形成二维微腔谐振，继而实现光增益和激射，其具有高功率、单纵模等优异特性。基于氮化镓基蓝光激光器结构和速率方程调制理论，对异质结构光子晶体面发射激光器进行了动态调制性能分析。通过仿真计算得出，在所研究的激光器结构参数下，阈值电流为 1.76 mA，最大 3 dB 调制带宽为 42 GHz，最低数据发送能耗为 62.78 pJ•bit^{-1}，展示出了该结构激光器的基础性能和高速调制特性，为具有大调制带宽的蓝光激光器的设计提供了参考。

关键词 激光器；光子晶体面发射激光器；速率方程；异质结构；3 dB 调制带宽；发送能耗

中图分类号 TN248 **文献标志码** A **DOI**：10.3788/CJL230499

1 引 言

经过几十年的发展，激光器的理论研究和实际应用都取得了丰硕的成果。自从光子晶体结构在 1987 年被提出之后[1]，激光器的发展就拥有了新的平台。光子晶体谐振腔具有能耗低、效率高、能够任意地控制光的发射和传播的优点，因此可以用来制作具有高性能的光学器件。

传统的边发射型激光器（EELs）[2-3]具有高输出功率且易波导集成，所以应用于长距离的电信通信，但是其具有大线宽、大腔体积和截面处产生光学损伤等缺点。垂直腔面发射激光器（VCSELs）[4-7]主要用于高速光互连，但是在大功率下工作且激光器发光区直径大于 5 μm 的时候，就容易产生多模，而且其使用的分布式布拉格反射器（DBR）的高电阻和电流阻塞氧化物层的大电容导致了较大的电阻电容常数（RC 常数），这也将其 3 dB 调制带宽限制在 30 GHz 以内[4]。光子晶体面发射激光器（PCSELs）在 1999 年首次被报道[8]。PCSELs 可以实现大面积单模激射，并且具有高功率、低阈值的优点，在光通信、激光雷达、激光打印等领域中有广阔的应用前景[9-13]。目前 GaAs、InP 基 PCSELs 由于其成熟和优异的性能，已得到应用[14-16]。在高速调制研究方面，2020 年，Inoue 等[17]设计的 GaAs 基光子晶体面发射激光器，可以在发光区直径为 9 μm 时实现单模激光，拥有超过 40 GHz 的 3 dB 调制带宽。InP 基异质结 PCSELs 可以实现高效的单模激光，具有低的阈值电流并且具有更大的机械和热稳定性，在提高限制因子的情况下，3 dB 调制带宽可以达到 27.18 GHz[18]。

随着三五族外延生长技术和器件结构设计理论的进步，GaN 基激光器在近些年得到了高效的开发[19-26]。GaN 基有源材料能灵活可调地覆盖紫外到绿光的任意波段，从而基于此的激光器与成熟的 GaAs 基、InP 基激光器形成了互补。传统 PCSELs 通常要求激光发光区直径大于 300 μm，以获得足够大的面内反馈，从而获得低损耗相干激光。本文提出的 GaN 蓝光激光器采用异质型结构光子晶体微腔，在拥有相对高的品质因数（Q）的同时，可以实现更小的激光面积和模场体积（V_m），从而减小器件电容，增加光子密度和弛豫振荡频率，因此具有大带宽调制特性。

本文瞄准激光器的高速调制特性，针对 PCSELs 展开分析讨论。首先通过速率方程模型得出激光器的阈值电流、3 dB 调制带宽和输出功率的公式，然后对 GaN 基异质结构 PCSELs 进行动态性能分析，得出激光器的特性数据，并与其他激光器进行对比，以验证此设计结构的性能。研究结果为 GaN 基激光器和光子晶体面发射激光器的动态响应性能分析及高速激光器件设计提供了参考。

2 光子晶体面发射激光器的调制理论

2.1 速率方程

为了对激光器进行调制性能分析，首先从经典的速率方程开始。GaN 基激光器通常有一个 p 型 AlGaN 包覆层，形成了一个单独的约束异质结构（SCH）。在

收稿日期：2023-02-07；**修回日期**：2023-04-04；**录用日期**：2023-04-11；**网络首发日期**：2023-04-21

基金项目：信息光子学与光通信国家重点实验室（北京邮电大学）开放基金（IPOC2021B03）、区域光纤通信网与新型光通信系统国家重点实验室开放基金（2023GZKF018）、国家自然科学基金（11974188）

通信作者：*liuqf@njupt.edu.cn

考虑载流子到达有源区的输运时间也就是输运效应的情况下，针对异质结构有源区中载流子的流动及其最终的复合建立了速率方程模型。一个是势垒区内的载流子密度(N_{SCH})，另一个是量子阱有源区的载流子密度(N_{QW})，这样建立的速率方程模型就可以用来模拟PCSELs，具体公式[27-29]为

$$\frac{\mathrm{d}N_{SCH}}{\mathrm{d}t}=\eta_i\left(\frac{I}{qV_{SCH}}\right)-\left(\frac{N_{SCH}}{\tau_s}\right)+\left(\frac{\Gamma_q N_{QW}}{\tau_e}\right), \tag{1}$$

$$\frac{\mathrm{d}N_{QW}}{\mathrm{d}t}=\left(\frac{N_{SCH}}{\Gamma_q\tau_s}\right)-\left(\frac{N_{QW}}{\tau_e}\right)-\left(AN_{QW}+BN_{QW}^2+CN_{QW}^3\right)-v_gG\left(N_{QW}\right)N_p, \tag{2}$$

$$\frac{\mathrm{d}N_p}{\mathrm{d}t}=\Gamma v_gG\left(N_{QW}\right)N_p+\Gamma\beta BN_{QW}^2-\frac{N_p}{\tau_p}, \tag{3}$$

式中：N_{SCH}为SCH区载流子密度；t为时间；η_i为电流的注入效率，即注入电流能在有源区产生载流子的比率；I为注入电流；q为正电荷的电荷量；V_{SCH}为SCH区的体积；$\eta_i\left(\frac{I}{qV_{SCH}}\right)$为SCH区每单位体积内的注入电子速率；$\tau_s$为光子从量子阱区到SCH区的热电子发射寿命；$N_{SCH}/\tau_s$为载流子从SCH区到量子阱有源区的损耗效率；$\Gamma_q$为量子阱有源区与SCH区的体积比，$\Gamma_q=V/V_{SCH}$，其中$V$为量子阱有源区体积；$N_{QW}/\tau_e$为载流子从量子阱到SCH区的损耗速率；$N_{QW}$为量子阱区载流子密度；$\tau_e$为SCH区载流子的扩散时间常数；$\Gamma_qN_{QW}/\tau_e$为净受激复合项；$A$为非辐射复合系数；$B$为双分子复合系数；$C$为俄歇复合系数；$AN_{QW}$为缺陷复合速率；$BN_{QW}^2$为自发复合速率；$CN_{QW}^3$为俄歇复合速率；$v_g$为光子的群速度；$G\left(N_{QW}\right)$为载流子相关增益；$N_p$为光子密度；$\Gamma$为限制因子，$\Gamma=V/V_p$，其中$V_p$为光子区的体积；$v_gG\left(N_{QW}\right)N_p$为光子激发的电子空穴对的净复合；$\beta$为自发发射因子；$\tau_p$为光子寿命；$N_p/\tau_p$为光子损耗速率。

载流子相关增益方程表示为

$$G\left(N_{QW}\right)=\left(\frac{g_0}{1+DN_p}\right)\ln\left(\frac{N_{QW}+N_s}{N_{tr}+N_s}\right), \tag{4}$$

式中：g_0为增益斜率常数，$g_0=v_ga_0$，a_0为常数；D为增益压缩因子；N_{tr}为透明载流子密度；N_s为外加的移位值。

τ_s和τ_e的表达式分别为

$$\tau_s=\frac{1}{2}\left(\frac{t_{SCH}^2}{2D_p}+\frac{t_{SCH}^2}{2D_n}\right), \tag{5}$$

$$\tau_e=\left(\frac{2\pi m\cdot t_{QW}^2}{k_BT}\right)^{1/2}\exp\left(\frac{E_b}{k_BT}\right), \tag{6}$$

式中：t_{SCH}为有源层厚度；D_p和D_n分别为p区和n区的扩散常数；m为质量；t_{QW}为整个量子阱层的厚度；k_B为玻尔兹曼常数；T为绝对温度；E_b为能量。

2.2 阈值电流

在达到阈值之前，载流子积聚在激光腔中，但没有激光发射出来。当注入电流大于阈值电流时，激光器才会工作。令$\frac{\mathrm{d}N_{SCH}}{\mathrm{d}t}=0$，$\frac{\mathrm{d}N_{QW}}{\mathrm{d}t}=0$，可得

$$N_{SCHth}=\Gamma_q\tau_s\left[\left(\frac{N_{QWth}}{\tau_e}\right)-\left(AN_{QWth}+BN_{QWth}^2+CN_{QWth}^3\right)-v_gG\left(N_{QW}\right)N_p\right], \tag{7}$$

$$N_{QWth}=\left(N_{tr}+N_s\right)\exp\left[\frac{G_{th}\left(1+DN_p\right)}{g_0}\right]-N_s, \tag{8}$$

式中：N_{SCHth}为阈值SCH区载流子密度；N_{QWth}为阈值量子阱有源区的载流子密度；G_{th}为阈值载流子的相关增益。

所以PCSELs的阈值电流可表示为

$$I_{th}=\frac{qV_{SCH}}{\eta_i}\left[\left(\frac{N_{SCHth}}{\tau_s}\right)-\left(\frac{\Gamma_qN_{QWth}}{\tau_e}\right)\right], \tag{9}$$

式中：I_{th}为阈值电流。

由式(9)可以看出，阈值电流与模场体积成正比，体积越小，激光器的阈值电流越小。

2.3 调制带宽

当考虑输运效应时，增益微分变为

$$a=\frac{\partial g}{\partial N}=\frac{1}{\chi}\left(\frac{g_0}{1+DN_p}\right)\left(\frac{1}{N_{QW}+N_s}\right), \tag{10}$$

式中：a为增益微分；g为增益；N为载流子密度；χ为输运因子，$\chi=1+\frac{\tau_s}{\tau_e}$。

而在速率方程的微分分析中，光子增益微分为

$$a_p=\frac{DG\left(N_{QW}\right)}{1+DN_p}, \tag{11}$$

$$\frac{1}{\tau_1}=AN^2+BN^2+CN^2, \tag{12}$$

式中：a_p为光子增益微分；τ_1为微分载流子寿命。

在远高于阈值的地方，N_p足够大，各速率系数[17]就可以简化为

$$\gamma_{NN}=\frac{1}{\tau_1}+v_gaN_p, \tag{13}$$

$$\gamma_{NP}=\frac{1}{\Gamma\tau_p}-v_ga_pN_p, \tag{14}$$

$$\gamma_{PN}=\Gamma v_gaN_p, \tag{15}$$

$$\gamma_{PP}=\Gamma v_ga_pN_p, \tag{16}$$

式中：γ_{NN}、γ_{NP}、γ_{PN}、γ_{PP}为速率系数。

则弛豫振荡频率和阻尼因子的表达式分别为

$$\omega_R^2=\frac{1}{\chi}\left(\gamma_{NN}\gamma_{NP}+\gamma_{PN}\gamma_{PP}\right), \tag{17}$$

$$\gamma=\frac{1}{\chi}\gamma_{NN}+\gamma_{PP}, \tag{18}$$

式中：ω_R为弛豫振荡频率；γ为阻尼因子。

调制响应为

$$H(\omega)=\eta_i\eta_o\frac{h\upsilon}{q}\times\frac{\omega_R^2}{\omega_R^2-\omega^2+j\omega\gamma}\times\frac{1}{1+j\omega\tau_s},\tag{19}$$

式中：ω为振荡频率；$H(\omega)$为调制响应；η_o为输出效率；h为普朗克常量；υ为光的频率。

弛豫振荡频率为

$$f_r=\frac{1}{2\pi}\sqrt{\frac{N_p v_g a}{\tau_p\chi}}=\frac{1}{2\pi}\sqrt{\frac{N_p v_g a(2\pi c)}{Q\lambda\chi}}=\frac{1}{2\pi}\sqrt{\frac{\eta_i v_g a}{q\chi V_{SCH}}}\left(\sqrt{I_a-I_{th}}\right),\tag{20}$$

式中：c为光速；f_r为弛豫振荡频率；λ为谐振波长；I_a为注入电流。

可得 3 dB 调制带宽为

$$f_{3\,dB}=\sqrt{1+\sqrt{2}}\,f_r,\tag{21}$$

式中：$f_{3\,dB}$为 3 dB 调制带宽。

从式(21)看出 3 dB 调制带宽与弛豫振荡频率成正比，而光子密度与弛豫振荡频率成正比，有源区体积与弛豫振荡频率成反比，因此可以得出，大的光子密度和小的有源区体积可以实现高的调制带宽。

2.4　输出功率

从载流子密度方程分析可得

$$\frac{dN}{dt}=\eta_i\frac{I}{qV}-\frac{N}{\tau}-v_g gN_p,\tag{22}$$

式中：τ为载流子寿命；$\frac{N}{\tau}=AN^2+BN^2+CN^2$。

由于激光器工作在阈值之下时$v_g gN_p$不起作用，令式(22)为 0，可得在阈值以下且接近阈值时的稳态载流子速率方程为

$$\eta_i\frac{I_{th}}{qV}=\frac{N_{th}}{\tau},\tag{23}$$

式中：N_{th}为载流子阈值密度。当高于阈值时，把式(23)代入式(22)中，可以得到

$$\frac{dN}{dt}=\eta_i\frac{(I-I_{th})}{qV}-v_g gN_p,\ I>I_{th}。\tag{24}$$

当半导体激光器工作在直流稳态的情况下时，载流子密度达到稳定状态，这时有

$$\frac{dN}{dt}=0。\tag{25}$$

假定η_i与阈值以上电流无关，就可以得出$g=g_{th}$时阈值以上的稳态光子密度，即

$$N_p=\eta_i\frac{(I-I_{th})}{q\upsilon_g g_{th}V},\tag{26}$$

式中：g_{th}为阈值增益。

而输出功率正比于光子密度N_p，所以经过替换后可得到输出功率的公式为

$$P_{out}=\eta_d\left(\frac{h\upsilon}{q}\right)(I-I_{th}),\tag{27}$$

式中：P_{out}为输出功率；η_d为微分量子效率，$\eta_d=\eta_i\eta_o$。当注入电流一定时，阈值电流I_{th}越小，输出功率越大。

当$\eta_o=1$时，由式(27)可得

$$P_{out}=\eta_i\left(\frac{hc}{q\lambda}\right)(I-I_{th})。\tag{28}$$

可以看出，激光器的输出功率与注入电流成正比，考虑到激光器的辐射复合时间和光子寿命，当阈值电流变低时，就可以得到较大的输出功率。

3　光子晶体面发射蓝光激光器的性能分析

普通 PCSELs 具有大面积(一般发光区直径大于 300 μm)的低损耗面内反馈光子晶体区，这会带来大的电容，极大限制调制带宽。本激光器结构将光子晶体层分为核心层和包层，核心层的空气孔半径略大于包层空气孔半径。这样可以在有效减小模场体积的同时减小面内损耗，实现高的Q/V_m光场谐振，降低激光器电容，提高调制带宽。

本文利用第 2 节公式进行编程，从而获得所有关系图，仿真建模流程图如图 1 所示。首先利用有限时域差分(FDTD)法建立激光器模型，然后优化激光器的结构参数，从而获得高的Q/V_m。利用第 2 节阈值电流、调制带宽和激光器输出功率的公式，编写 MATLAB 代码，同时将激光器的参数值代入代码，最终得到 3 dB 调制带宽、输出功率和最低能量消耗的关系图。

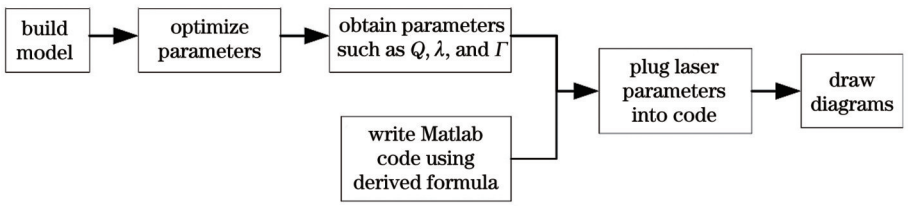

图 1　仿真建模流程图

Fig. 1　Flow chart of simulation modeling

首先固定激光器的其他所有参数，只改变光子晶体微腔的谐振区直径，范围为 10～300 μm，就可计算得到激光器有源区体积为 2～636 μm³。利用式(9)直接计算得到的阈值电流(计算值)；令式(3)为 0，当设置光输出功率为 1～10 mW 时，就可以在－1～10 区间仿真计算出零点；利用功率与电流的关系式(27)，得

出阈值电流仿真值。如图 2(a)所示，阈值电流随着激光器体积的减小而减小，仿真结果和计算结果吻合很好。在 10 μm 有源区直径下进行研究，改变激光器的品质因子 Q 值，当 Q 开始增加时，阈值电流减小，当 Q 进一步增加时，阈值电流趋于稳定，如图 2(b)所示。

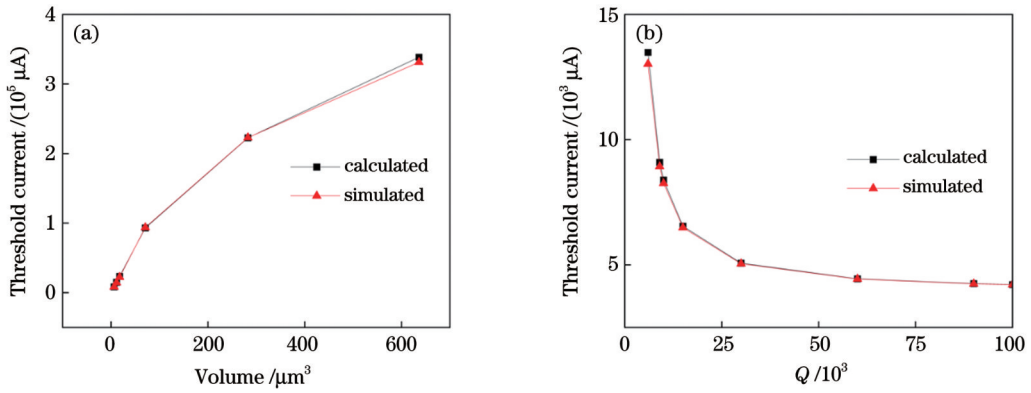

图 2　阈值电流的计算值和仿真值。(a)阈值电流随有源区体积的变化；(b)阈值电流随品质因子的变化

Fig. 2　Calculated and simulated values of threshold current. (a) Threshold current versus volume of active region; (b) threshold current versus quality factor

激光器的层结构采用传统的 GaN 基有源蓝光结构，基于严格耦合波分析法(RCWA)和 FDTD 法，对微腔结构参数进行相互验证设计，通过 FDTD 仿真，计算得到 λ、Γ、Q 等参数。得出该异质结构微腔的谐振波长 λ 为 452.823 nm，相应的量子阱的限制因子 Γ 为 0.13。当有源区直径固定为 10 μm 时，激光器的有源区体积为 2.1206 μm^3，品质因子 Q 为 7076。GaN 光子晶体面发射激光器的具体结构如图 3 所示，参数如表 1 所示。

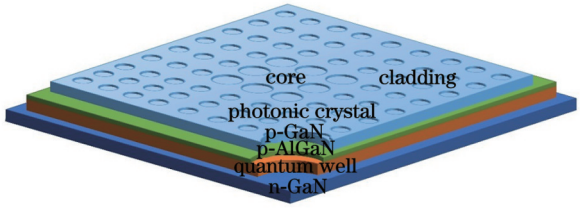

图 3　GaN 光子晶体面发射激光器的结构示意图

Fig. 3　Structural diagram of GaN photonic crystal surface-emitting laser

此时通过仿真计算可以得到激光器的调制带宽、输出功率及能耗，如图 4 所示。其中图 4(b)为输出功率与注入电流的关系图，可得阈值电流为 1.76 mA。图 4(c)为激光器能耗随注入电流的变化图，可得在 2.4 mA 偏置电流下，直接调制的最低数据发送能耗为 62.78 pJ·bit^{-1}，此时 3 dB 调制带宽为 6.166 GHz，输出功率为 0.795 mW。根据图 4(a)可知，随着注入电流的增大，3 dB 调制带宽峰值可达 42 GHz。

表 1　氮化镓光子晶体面发射激光器的结构及相关参数

Table 1　Structure and parameters of GaN photonic crystal surface-emitting laser

Parameter	Content
Composition of photonic crystal layer	Hole radius of 60 nm and 30 cycles for core region, hole radius of 52 nm and 130 cycles for cladding region
Thickness of photonic crystal layer /nm	20
p-GaN layer thickness /nm	80
p-AlGaN layer thickness /nm	35
Composition of GaN/InGaN quantum well layer	9 pairs GaN/InGaN
Thickness of GaN/InGaN quantum well layer /nm	10/3
n-GaN layer thickness /nm	100
Active zone volume V /μm^3	2.1206
Resonant wavelength λ /nm	452.823
Quantum well restriction factor Γ	0.13
Quality factor Q	7076

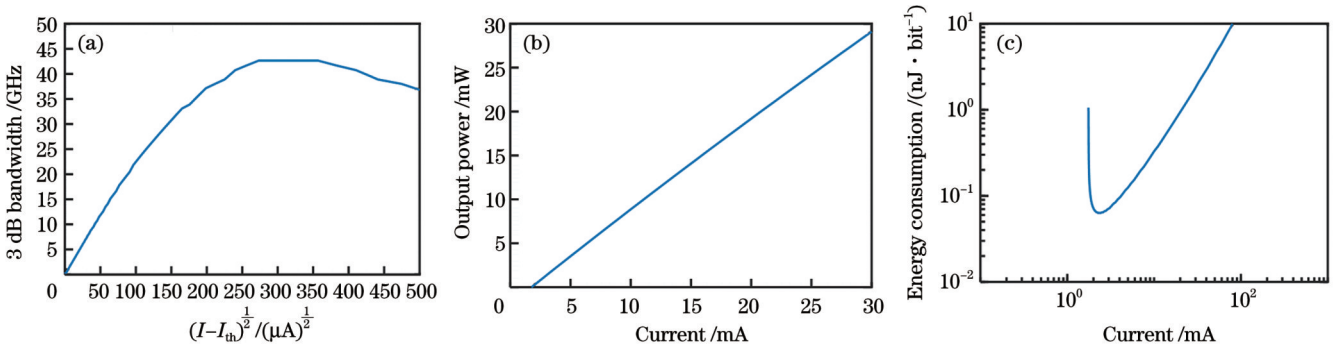

图 4 实验结果。(a) 3 dB 调制带宽;(b)输出功率随注入电流的变化;(c)能量消耗随注入电流的变化

Fig. 4 Experimental results. (a) 3 dB modulation bandwidth; (b) output power versus injection current; (c) energy consumption versus injection current

表 2 所示为 PCSELs、VCSELs、波长级有源区掩埋型光子晶体缺陷型激光器(LEAP)、纳米梁激光器、Si 基分布式反馈(DFB)激光器的调制带宽等参数。Inoue 等[17]采用基于 GaAs 的双晶格光子晶体结构,实现了 0.5 mA 阈值电流,最大 3 dB 调制带宽为 41.85 GHz。InP/InGaAsP 基 LEAP[30]的体积为 0.18 μm^3,在高速调制条件下,最低能量消耗为 13 fJ·bit^{-1},3 dB 调制带宽为 5.5 GHz,输出功率为 0.44 mW。光子晶体纳米梁激光器[31]一般体积很小,当体积为 0.01 μm^{3}时,阈值电流只有 0.49 μA。在 0.88 μA 偏置电流和 7.58 GHz 调制带宽下,得到的最低能量消耗为 0.06 fJ·bit^{-1},最大 3 dB 调制带宽也可以达到 20.5 GHz。在文献[4]中,VCSELs 的阈值电流为 0.14 mA,最大 3 dB 调制带宽约为 20 GHz,最低能量消耗为 286 fJ·bit^{-1}。Takeda 等[32]通过减小有源区体积,制备了体积为 0.04725 μm^{3}的 InP 基 LEAP,当偏置电流为 10.5 μA 时,实现了最低能量消耗 1 fJ·bit^{-1}。而 Si 基 DFB 激光器在阈值电流为 160 mA 的情况下,调制速度被限制在 12.5 Gbit·s^{-1},此时最低能量消耗为 27 pJ·bit^{-1}[33]。

表 2 已报道的激光器特性数据比较

Table 2 Comparison of reported laser characteristic data

Laser	Laser volume / μm^3	Threshold current / mA	Maximum 3 dB modulation bandwidth / GHz	Minimum sending energy consumption / (fJ·bit^{-1})	Output power / mW	Research type
Proposed laser	2.1206	1.76	42	62780	0.795	Theoretical prediction
GaAs-based dual-lattice PESELs[17]		0.5	41.85			Theoretical prediction
LEAP[30]	0.18		5.5	13	0.44	Experiment
Photonic crystal nanobeam lasers[31]	0.01	0.00049	20.5	0.06		Theoretical prediction
VCSELs[4]		0.14	20	286	10	Experiment
LEAP[32]	0.04725	0.0041		1		Experiment
Si-based DFB lasers[33]		160		27 000	17	Experiment

LEAP 和纳米梁激光器的模场体积小,所以激光面积小,具有低的发送能耗,但是功率也会小。本文激光器具有较大的体积、较高的 3 dB 调制带宽和更大的输出功率,可以实现大面积单模激射。VCSELs 具有高的串联电阻和电容,直接影响器件的高速性能,所以最大 3 dB 调制带宽被限制在 30 GHz。PCSELs 为实现更低发送能耗的通信提供了可能,可以弥补目前激光器应用的不足。本文激光器与报道的 GaAs 基双晶格 PCSELs 相比,阈值电流和最大 3 dB 调制带宽都在同一水平,说明采用 GaN 基的光子晶体面发射激光器同样可以实现优异的性能。GaN 基激光器可以灵活可调地覆盖紫光到绿光的任意波段,与成熟的 GaAs 基激光器形成了互补。

4 结 论

高输出功率、低阈值、大调制带宽是激光器的核心需求。首先根据激光器的速率方程模型理论,得出 PCSELs 的阈值电流、3 dB 调制带宽和输出功率的表达式。然后对一种氮化镓基光子晶体面发射激光器进行了基础性能和调制带宽性能分析,并与其他已报道的激光器进行了对比。所提的仿真计算和分析半导体激光器基础特性和动态调制特性的方法,为具有优异

特性和高速调制特性的PCSELs的设计提供了指导。

参 考 文 献

[1] Yablonovitch E. Inhibited spontaneous emission in solid-state physics and electronics[J]. Physical Review Letters, 1987, 58(20): 2059-2062.

[2] Ryu H Y, Kwon S H, Lee Y J, et al. Very low threshold photonic band edge lasers from free-standing triangular photonic crystal slabs [J]. Applied physics letters, 2002, 80(19): 3476-3478.

[3] Painter O, Lee R K, Scherer A, et al. Two-dimensional photonic band-gap defect mode laser[J]. Science, 1999, 284(5421): 1819-1821.

[4] Chang Y C, Coldren L A. Efficient, high-data-rate, tapered oxide-aperture vertical-cavity surface-emitting lasers[J]. IEEE Journal of Selected Topics in Quantum Electronics, 2009, 15(3): 704-715.

[5] Panajotov K, Prati F. VCSELs: fundamentals, technology and applications of vertical-cavity surface-emitting lasers[M]// Michalzik R. Springer series in optical sciences. Berlin: Springer, 2012.

[6] 项国洪, 贾思琪, 李德鹏, 等. 胶体量子点垂直腔面发射激光器的设计与仿真[J]. 中国激光, 2021, 48(19): 1901005.
Xiang G H, Jia S Q, Li D P, et al. Design and simulation of a colloidal quantum dot vertical-cavity surface-emitting laser[J]. Chinese Journal of Lasers, 2021, 48(19): 1901005.

[7] 潘智鹏, 李伟, 戚宇轩, 等. 光子晶体垂直腔面发射激光器的设计分析[J]. 光学学报, 2022, 42(14): 1414002.
Pan Z P, Li W, Qi Y X, et al. Design and analysis of photonic crystal vertical-cavity surface-emitting lasers[J]. Acta Optica Sinica, 2022, 42(14): 1414002.

[8] Imada M, Noda S, Chutinan A, et al. Coherent two-dimensional lasing action in surface-emitting laser with triangular-lattice photonic crystal structure[J]. Applied Physics Letters, 1999, 75(3): 316-318.

[9] Hsu M Y, Lin G, Pan C H. Electrically injected 1.3-μm quantum-dot photonic-crystal surface-emitting lasers[J]. Optics Express, 2017, 25(26): 32697-32704.

[10] Yoshida M, De Zoysa M, Ishizaki K, et al. Double-lattice photonic-crystal resonators enabling high-brightness semiconductor lasers with symmetric narrow-divergence beams[J]. Nature Materials, 2019, 18(2): 121-128.

[11] Sakata R, Ishizaki K, De Zoysa M, et al. Dually modulated photonic crystals enabling high-power high-beam-quality two-dimensional beam scanning lasers[J]. Nature Communications, 2020, 11(1): 1-10.

[12] Chen L R, Hong K B, Chen H L, et al. Vertically integrated diffractive gratings on photonic crystal surface emitting lasers[J]. Scientific Reports, 2021, 11(1): 1-7.

[13] Hong Y H, Miao W C, Hsu W C, et al. Progress of photonic-crystal surface-emitting lasers: a paradigm shift in LiDAR application[J]. Crystals, 2022, 12(6): 800.

[14] Ishizaki K, de Zoysa M, Noda S. Progress in photonic-crystal surface-emitting lasers[J]. Photonics, 2019, 6(3): 96.

[15] Belyanin A A, Smowton P M. Novel in-plane semiconductor lasers XIX[J]. Proceedings of SPIE, 2020, 11301: 1130101.

[16] Reuterskiöld Hedlund C, Martins De Pina J, Kalapala A, et al. Buried InP/airhole photonic-crystal surface-emitting lasers[J]. Physica Status Solidi (a), 2021, 218(3): 2000416.

[17] Inoue T, Yoshida M, Zoysa M D, et al. Design of photonic-crystal surface-emitting lasers with enhanced in-plane optical feedback for high-speed operation[J]. Optics Express, 2020, 28(4): 5050-5057.

[18] Peng C Y, Cheng H T, Hong Y H, et al. Performance analyses of photonic-crystal surface-emitting laser: toward high-speed optical communication[J]. Nanoscale Research Letters, 2022, 17(1): 90.

[19] Sun Y, Zhou K, Sun Q, et al. Room-temperature continuous-wave electrically injected InGaN-based laser directly grown on Si [J]. Nature Photonics, 2016, 10(9): 595-599.

[20] Kuramoto M, Kobayashi S, Akagi T, et al. Enhancement of slope efficiency and output power in GaN-based vertical-cavity surface-emitting lasers with a SiO_2-buried lateral index guide[J]. Applied Physics Letters, 2018, 112(11): 111104.

[21] Wang J, Feng M X, Zhou R, et al. Continuous-wave electrically injected GaN-on-Si microdisk laser diodes[J]. Optics Express, 2020, 28(8): 12201-12208.

[22] 梁锋, 赵德刚, 江德生, 等. 光场分布对GaN基绿光激光器的影响[J]. 中国激光, 2020, 47(7): 0701018.
Liang F, Zhao D G, Jiang D S, et al. Influence of light field distribution on Gan-based green laser[J]. Chinese Journal of Lasers, 2020, 47(7): 0701018.

[23] Elafandy R T, Kang J H, Mi C, et al. Study and application of birefringent nanoporous GaN in the polarization control of blue vertical-cavity surface-emitting lasers[J]. ACS Photonics, 2021, 8 (4): 1041-1047.

[24] Hong K B, Chang T C, Hjort F, et al. Monolithic high-index contrast grating mirror for a GaN-based vertical-cavity surface-emitting laser[J]. Photonics Research, 2021, 9(11): 2214-2221.

[25] Yang J, Zhao D G, Liu Z S, et al. Room temperature continuous-wave operated 2.0-W GaN-based ultraviolet laser diodes[J]. Optics Letters, 2022, 47(7): 1666-1668.

[26] Emoto K, Koizumi T, Hirose M, et al. Wide-bandgap GaN-based watt-class photonic-crystal lasers[J]. Communications Materials, 2022, 3(1): 1-8.

[27] Matsuo S, Kakitsuka T. Low-operating-energy directly modulated lasers for short-distance optical interconnects[J]. Advances in Optics and Photonics, 2018, 10(3): 567-643.

[28] Coldren L A, Corzine S W, Mašanović M L. Diode lasers and photonic integrated circuits[M]. Hoboken: John Wiley & Sons, Inc., 2012.

[29] Alahyarizadeh G, Aghajani H, Mahmodi H, et al. Analytical and visual modeling of InGaN/GaN single quantum well laser based on rate equations[J]. Optics & Laser Technology, 2012, 44(1): 12-20.

[30] Matsuo S, Shinya A, Kakitsuka T, et al. High-speed ultracompact buried heterostructure photonic-crystal laser with 13 fJ of energy consumed per bit transmitted[J]. Nature Photonics, 2010, 4(9): 648-654.

[31] Gadiyaram N K, Coleman J, Zhou W D. Towards attojoule operation of semiconductor quantum well lasers[C]//2020 IEEE Photonics Conference (IPC), September 28-October 1, 2020, Vancouver, BC, Canada. New York: IEEE Press, 2020.

[32] Takeda K, Fujii T, Shinya A, et al. 1-fJ/bit direct modulation of photonic-crystal lasers[C]//2018 European Conference on Optical Communication (ECOC), September 23-27, 2018, Rome, Italy. New York: IEEE Press, 2018.

[33] Descos A, Jany C, Bordel D, et al. Heterogeneously integrated Ⅲ-V/Si distributed Bragg reflector laser with adiabatic coupling [C]//39th European Conference and Exhibition on Optical Communication (ECOC 2013), September 22-26, 2013, London. London: IET, 2013.

Analysis of High-Speed Modulation Performance of Photonic Crystal Surface-Emitting Blue Lasers

Zhou Yang, He Shumin, Shen Wei, Liu Qifa*

College of Communications and Information Engineering, Nanjing University of Posts and Telecommunications, Nanjing 210003, *Jiangsu, China*

Abstract

Objective With the development of a new generation of electronic communication technology, data traffic for transmitting information is increasing, thereby driving the development of optical communication technology for higher speed, larger capacity, and lower power consumption. Photonic crystal surface-emitting lasers (PCSELs) are the key devices in this field that have a wide range of potential applications. PCSELs exhibit outstanding features, such as large-area single-mode excitation, arbitrary beam shaping and polarization, and high power. Simultaneously, GaN compounds can be flexible and adjustable to cover any wavelength band from ultraviolet (UV) to green, thereby the laser based on this is complementary to the mature GaAs- and InP-based lasers. Using a photonic crystal heterostructure design can improve the performance of a laser, particularly for achieving large bandwidths. In this study, the expressions for the threshold current, 3 dB modulation bandwidth, and output power of PCSELs are derived using the rate equation model, and the fundamental and modulation performances of a GaN-based photonic crystal surface emission laser are analyzed and compared with those of other reported lasers. This investigation lays the foundation for the design of blue-light lasers with large modulation bandwidths.

Methods In this study, we first derive expressions for the threshold current, 3 dB modulation bandwidth, and output power of PCSELs using the classical rate equation model to lay the foundation for subsequently writing the code in MATLAB. GaN-based PCSELs are selected for modulation analysis, and the core parameters of the laser are derived after strict finite-domain difference (FDTD)-based calculations and verified using the ensemble wave analysis method (RCWA). The MATLAB codes are written using the derived equations and the laser parameter values are substituted into this code to obtain a plot in which the 3 dB modulation bandwidth, output power, and minimum energy consumption are indicated. The relationship between the calculated and simulated values of the threshold current is investigated by changing a single parameter using the control-variable method. Finally, properties such as the modulation bandwidth are compared with those of vertical cavity surface-emitting, wavelength-level active region buried photonic crystal defect, nanobeam, and Si-based distributed feedback lasers to highlight the advantages of GaN-based heterostructure PCSELs.

Results and Discussions We first derive the expressions for the threshold current, 3 dB modulation bandwidth, and output power of PCSELs. The calculated and simulated values of the threshold current can be obtained by changing the volume of the active region of the laser, and the values show good agreement. When the quality factor (Q) of the laser increases, the calculated and simulated values of the threshold current decrease, and when Q increases further, the calculated and simulated values of the threshold current converge to remain constant (Fig. 2). Subsequently, the FDTD calculations of the PCSELs (Fig. 3) yield a threshold current of 1.76 mA for the laser and a minimum data transmission energy consumption of 62.78 pJ/bit for direct modulation at 2.4 mA bias current when the 3 dB modulation bandwidth is 6.166 GHz and the output power is 0.795 mW. With an increase in the injection current, the 3 dB modulation bandwidth peaks at 42 GHz (Fig. 4). Finally, the threshold currents, maximum modulation bandwidths, minimum energy loss values, and output powers of various types of lasers that have been reported (Table 2) are listed to compare their advantages and disadvantages with those of PCSELs, and it is observed that GaN-based PCSELs can make up the shortcomings of the current laser applications.

Conclusions This study focuses on the modulation, threshold, and output power characteristics of PCSELs. We first derive the expressions for the threshold current, 3 dB modulation bandwidth, and output power of the PCSELs based on the rate equation model theory of the laser. Subsequently, the fundamental performance and modulation bandwidth performance of a GaN-based photonic crystal surface emission laser are analyzed, and the threshold current of 1.76 mA, the maximum 3 dB modulation bandwidth of 42 GHz, and the minimum data transmission energy consumption of 62.78 pJ/bit are obtained by simulation, thus demonstrating the fundamental performance and high-speed modulation characteristics of the proposed GaN-PCSEL with the studied structure parameters. This study provides the basic performance and high-speed modulation characteristics of the laser and the comparisons with other reported lasers. In this study, a methodology for simulating and analyzing the fundamental and dynamic modulation characteristics of semiconductor lasers is developed, which provides a theoretical basis and guidance for the design of PCSELs with excellent high-speed modulation characteristics.

Key words lasers; photonic crystal surface-emitting laser; rate equation; heterostructure; 3 dB modulation bandwidth; transmission energy cost